CHEMICAL ENGINEERING TRANSACTIONS
VOL. 59, 2017
A publication of AIDIC
The Italian Association of Chemical Engineering
Online at www.aidic.it/cet
Guest Editors: Zhuo Yang, Junjie Ba, Jing Pan

ISBN 978-88-95608- 49-5; **ISSN** 2283-9216
DOI: 10.3303/CET1759163

Chemical and Mineralogical Study on Bastnaesite Dominated Rare Earth Ores

Yang Liu[a, b]

[a]Hunan Provincial Key Laboratory of Shale Gas Resource Utilization, Hunan University of Science and Technology, Xiangtan 411201, China
[b]Key Laboratory of Metallogenic Prediction of Nonferrous Metals and Geological Environmental Monitoring (Central South University), Ministry of Education, Changsha 410083, China
liuyang2585899@163.com

The process mineralogy characteristics, such as the chemical composition of the ores, the chemical phase of the rare earth, the mineral components and contents, the occurrence states of the main minerals, the disseminated grain size of the rare earth minerals, and the liberation analysis of the rare earth minerals, were studied in detail with the methods of lens-below identification, mineral liberation analyzer (MLA), scanning electron microscope, X-ray diffraction, chemical elements analyses, and the chemical phase analyses. The results show that the main rare earth mineral of the ores was bastnaesite (including parisite), which took up 87% of the total. Bastnaesite (parisite) was mainly disseminated in sparse and scattered forms along the edge or within the intergranular spaces of dolomite, celesite, apatite and quartz. The statistical results of the disseminate grain size indicate that the grain size smaller than 0.038 mm took up 40.47%. The rare-earth miners were featured with tiny grain size, high degree of dispersion, and complicated intergrowth relationship with the disseminated minerals. According for these characteristics, fine milling procedure would be applied to obtain high grade rare earth ore concentrate.

1. Introduction

The rare-earth elements and their minerals hold an important position in national economy. China has been the biggest rare earth producer based on the word first reserves (Massar and Ruberti, 2013). The rare earth functional materials such as permanent magnetism of rubidium-iron-boron material (Yu et al., 2005; Xia et al., 2011; Liu et al., 2015), trichromatic phosphor (Hirajima et al., 2005; Yu et al., 2008; Al-waisawy et al., 2016), rare earth oil cracking catalyst (Sousa-Aguiar et al., 2013; Wallenstein et al., 2015) and rare earth polishing powder (Liu et al., 2013; Lucas et al., 2015; Zouaoui et al., 2016) etc., have widely been studied with the development of the science and technology. Rare earths are the exploitation direction of the new future materials, and also play a significant role in the conventional industries (Xu, 1996). The rare-earth elements mostly occur in the rare-earth minerals, including bastnaesite, parisite, monazite, and xenotime etc (Gu, 2003; Che and Yu, 2006; Frandrich et al., 2007). Bastnaesite is the main light rare earth mineral, and takes up the biggest share of the proved rare earth reserves in China (Zhang, 1989). Some minerals containing rare earth elements are another important source for rare earth resources, for example, apatite often contains cerium, lanthanum and rubidium elements, these elements usually occur in apatite as isomorphism form (Zhang et al., 2007; Zirner et al., 2015). Other rare earth containing minerals include fluorite, mica and pyrochlore etc (Jordens et al., 2013; Jaireth et al., 2014). The rare-earth ore discussed in this paper is bastnaesite dominated rare earth deposit, with some other minerals such as monazite and xenotime. The processing mineralogical parameters such as the occurrence state of the useful elements, the chemical composition of the ores, the liberation degree, and the disseminated characteristics of the rare-earth minerals were clarified by conducting the processing mineralogical studies using microscope, scanning electron microscope and mineral liberation analyzer (MLA). This study would provide detail mineralogical basis for rare earth ore beneficiation.

Please cite this article as: Yang Liu, 2017, Chemical and mineralogical study on bastnaesite dominated rare earth ores, Chemical Engineering Transactions, 59, 973-978 DOI:10.3303/CET1759163

2. Methods

2.1 X-ray diffraction

X-ray diffraction (XRD) was performed in order to obtain qualitative analysis of the starting materials, samples of the original unreacted ores were sent to Changsha Research Institute of Mining and Metallurgy, CO., LTD for qualitative mineralogical analysis. XRD patterns were obtained from slightly back-pressed powder samples on a Bruker D8 Advance using Cu Kα radiation (λ=1.5418 Å) at 40 KV, 25 mA, in the range 0°-65° (2θ). The samples were scanned at 1° (2θ) min-1 with steps of 0.02° (2θ). This section should describe in detail the study material, procedures and methods used.

2.2 Chemical phase analysis

The original ores were sent to Changsha Research Institute of Mining and Metallurgy, CO., LTD for chemical phase analysis. According to the differences in the lattice energy, density, hardness and solubility product of the ores, the specific chemical solvents and test methods were chosen to make the ores quantitatively and selectively dissolve, then all the minerals of the ores could be measured in the solvent.

2.3 Mineral liberation analyzer

Mineral liberation analyzer (MLA) is the high-speed automatic mineral parameters quantitative analysis system, especially has good results for low-grade rare earth minerals. In this study, MLA was used to analyze the mineral contents, disseminated grain sizes, and liberation degree of the rare-earth minerals. The micrograph and relative percentage content of each mineral were observed by the scanning electron microscope (SEM) and energy dispersive spectrum (EDS) equipped with MLA. The MLA used in this study is MLA650, with FEI Quanta650 (SEM), Bruker Quantax200 (EDS), and process mineralogical parameters automatic analysis software (MLA3.1).

3. Results and discussion

3.1 Chemical composition of the ores

The results of chemical elements analysis of the ores and chemical phase analysis of the rare earth are shown in Tables 1 and 2, respectively. The results indicate that the dressing recovery of rare earth elements is 2.84%, the gangue components was mainly CaO, SiO_2, and some minor SrO, MgO and BaO, the total contents of the gangue was approximately 55.44%. The rare-earth elements occurred in carbonatite rare earth minerals form, having distribution ratio at 89.08%, together with the rare-earth elements occurred in phosphate minerals, the total distribution ratio was 98.59%, which could be considered as the maximum theoretical recovery ratio of the rare-earth elements in dressing concentration process.

Table 1: Chemical composition of the ores (%)

Component	TREO	Pb	Zn	TFe	FeO	Fe_2O_3	SiO_2	Al_2O_3	CaO
Content	2.84	0.19	0.05	3.69	0.86	4.31	12.21	1.85	30.26
Component	MgO	BaO	SrO	K_2O	P	S	F	C	Ignition Lost
content	3.55	2.87	7.12	1.13	1.80	2.88	3.09	5.29	19.28

Table 2: The results of the chemical phase analysis(%)

Rare earth phase	REO (Carbonatite)	REO (Phosphate)	Others	Total
Content	2.53	0.27	0.04	2.84
Distribution Ratio	89.08	9.51	1.41	100.00

3.2 Mineral composition and contents

XRD pattern (Fig.1) reveals the mineral components of the ores. The weight contents of the main minerals in the ores were counted by MLA, and the results are shown in Table 3. As indicated, the primary rare earth minerals were bastnaesite (including parisite), monazite, and minor other rare earth minerals, such as xenotime, ancylite, calcium tornebohmite, and loveringite. The main rare metal mineral was pyrochlore (merely 0.02 w.t.%); metal sulfide (0.15 w.t.%) including pyrite, pentlandite, copper pyrite, and gelenite; iron minerals were mainly limonite, together with minor hydrohematite and magnetite. The main gangue minerals were dolomite and apatite, together with minor celesite, calcite, quartz and fluorite.

Table 3: The contents of the primary minerals in the ores (w.t.%)

Mineral	Bastnaesite & Parisite	Xenotime &Monazite	Iron Mineral	Ancylite	Calcium Tornebohmite	Loveringite &Pyrochlore	Silicate Mineral
Content	4.23	0.42	2.69	0.02	0.07	0.12	6.69
Mineral	Metal Sulfide	Dolomite &Calcite	Celesite &Barite	Quartz& Feldspar	Apatite	Fluorite	Others
Content	0.15	39.30	17.49	11.75	6.91	8.57	2.00

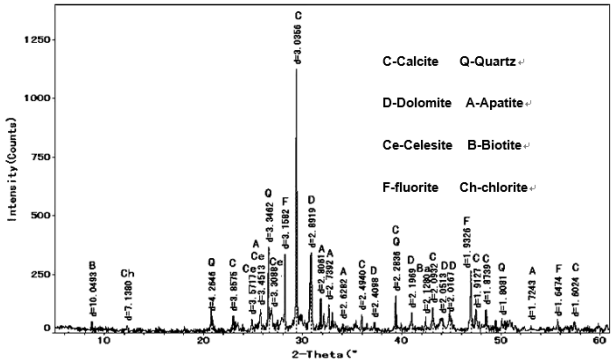

Figure 1: X-ray diffraction pattern of the ores

3.3 The occurrence of the main minerals

Bastnaesite, the primary rare earth mineral inores, was mainly idiomorphic, hypidiomorphic plate or granular, and few was in tiny petal shaped crystal stock form. Bastnaesite disseminated in sparse and scattered form along the intergranular, edge and crack of dolomite, celesite, apatite and quartz, especially having close intergrowth relationship with dolomite (Fig.2a). The contact boundary of bastnaesite and dolomite was straight and regular, the coarse grain size of the bastnaesite could reach 0.15mm, usually around 0.005~0.05mm (Fig.2b). Bastnaesite was characterized with fine grain size, high dispersion degree, complicated relationship with other minerals. The bastnaesite would still occurred in aggregate form even though for the fine grinding part. The results of SEM-EDS indicate that bastnaesite in the ores averagely contained La_2O_3 at 33.35%, Ce_2O_3 at 37.36%, Nd_2O_3 at 5.00%, CO_2 at 20.17% and F at 4.12%.

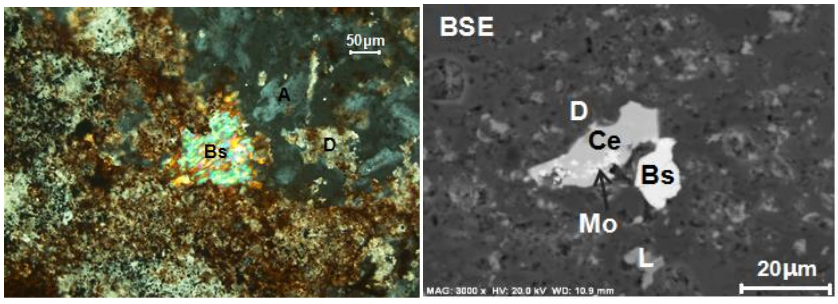

(a) (b)

Figure 2: (a) Bastnaesite (Bs) filled in the intergranular of dolomite (D) and apatite (A); (b) Hypidiomorphic particulate Bastnaesite (Bs) sporadically disseminated in dolomite (D), particulate monazite (phosphorus-rich area) was wrapped in celesite (Ce)

Parisite, very few content, and was occasionally observed, sporadically distributed in fine grain size form among dolomite, barite and celesite, the grain sizes were usually in the range of 0.005~0.03 mm. The results of SEM-EDS indicate that the parisite in the ores averagely contained La_2O_3 at 18.84%, Ce_2O_3 at 33.12%, Nd_2O_3 at 8.69%, CaO at 11.98%, CO_2 at 24.58% and F at 2.79%.

Monazite, having lower occurrence frequency than bastnaesite, was idiomorphic, hypidiomorphic-granular, and always distributed in irregular aggregate form within the intergranular of dolomite, calcite, apatite, barite and celesite (Fig.3a). Some monazite mix-intergrew with limonite, ferruginous matters and chlorite, the monazite usually had a fine grain size ranging from 0.01~0.15 mm (Fig.3b). The results of SEM-EDS indicate

that monazite had various types of rare earth elements, averagely contained La_2O_3 at 16.63%, Ce_2O_3 at 34.87%, Nd_2O_3 at 13.36%, Pr_2O_3 at 3.93%, Sm_2O_3 at 1.09%, Gd_2O_3 at 0.70%, ThO_2 at 0.59%, CaO at 0.55% and P_2O_5 at 28.28%.

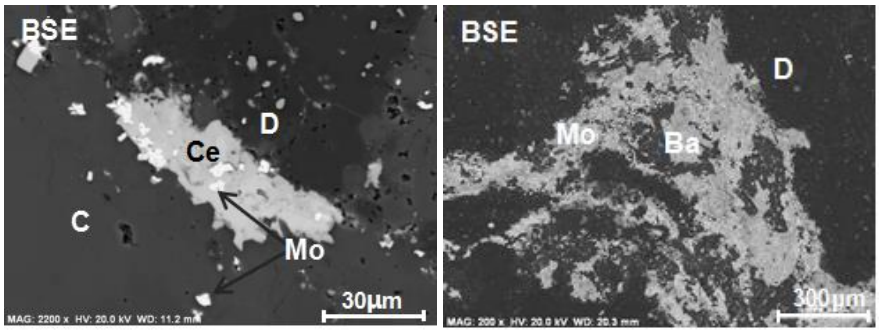

(a) (b)

Figure 3: (a) Particulate monazite (Mo) partly disseminated along the edge of celesite (Ce), partly wrapped in celesite, C-calcite; (b)Coarse monazite aggregate mix-intergrew with dolomite (D) and barite (Ba)

Xenotime, subordinated rare earth mineral in the ores, had quite low content, and was always observed together with monazite in the same ore block. Short column or granular xenotime sporadically occurred in dolomite or apatite, having the grain size at <0.01 mm (Fig.4a). The results of SEM-EDS indicate that xenotime contained Y_2O_3 at 45.00%, Gd_2O_3 at 3.95%, Dy_2O_3 at 8.62%, Er_2O_3 at 3.77%, SiO_2 at 3.06% and P_2O_5 at 35.6%.

Other rare earth minerals, including loveringite, ancylite and calcium tornebohmite, had low mineral contents. The occurrence states of these three minerals were similar, mainly fine-grain disseminated in the intergranular space of the gangue with the grain size at 0.01-0.03 mm.

Pyrochlore, the main rare earth metal mineral in the ores, mainly disseminated with idiomorphic and hypidiomorphic fine grain-sized texture in the intergranular spaces of dolomite and barite (Fig.4b). The pyrochlore scarcely disseminated with rare earth minerals, the grain size of which could be around 0.15 mm, generally at 0.005-0.03 mm. The results of SEM-EDS indicate that pyrochlore averagely contained Nb_2O_5 at 65.54%, La_2O_3 at 2.66%, Ce_2O_3 at 2.24%, ThO_2 at 4.65 %, Na_2O at 7.14, CaO at 15.16%, F at 2.61%.

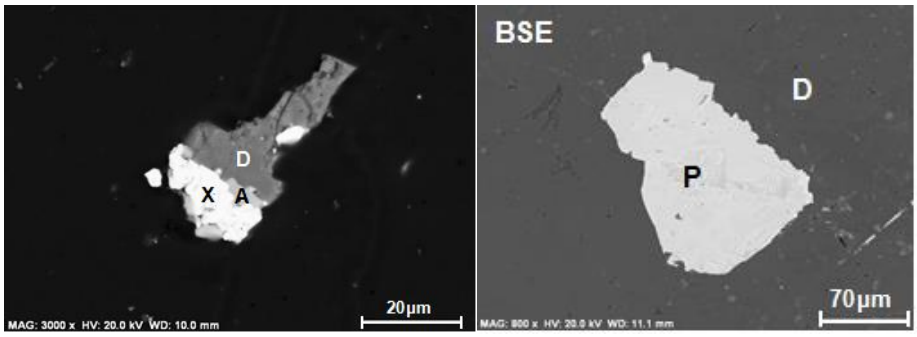

Figure 4: (a) Irregular granular xenotime (X) intergrew with apatite (A) and dolomite (D); (b) Granular pyrochlore (P) sporadically distributed in dolomite (D), BSE Image

Limonite, the main metallic mineral in the ores, had a wide distribution. It disseminated in gangue as irregular or fine veins, fine metasomatic relict pyrite could always be observed within the limonite. A few limonite came into being hematite due to the dehydration, limonite aggregates with the grain size at around 0.5 mm were observed in some areas of the mineral, the general grain size of the limonite ranged from 0.005-0.04 mm (Fig.5a).

Ferruginous matters, seen in most of the ore blocks, disseminated as powdered or skin-like structure along the edge, hole, cleavage and crack of the gangue. Ferruginous matters would usually be seen together with some rare-earth minerals such as monazite.

The common gangues in the ores were dolomite, apatite and some minor celesite, calcite, quartz and fluorite. Dolomite, having rhombic cleavage and idiomorphic, hypidiomorphic granular texture, always filled with fine rare earth miners and ferruginous matters along the edge, intergranular spaces and cracks. Celesite, the main silicates in the ores, usually distributed in intergranular spaces of dolomite, calcite and fluorite (Fig.5b). Apatite

generally occurred in crumby structure with radial pattern, rare earth minerals, silicates and ferruginous matters filled and replaced in the intergranular spaces and cracks of the apatite. Quartz and fluorite were both in irregular granular form along the edge, intergranular spaces and holes of the silicates.

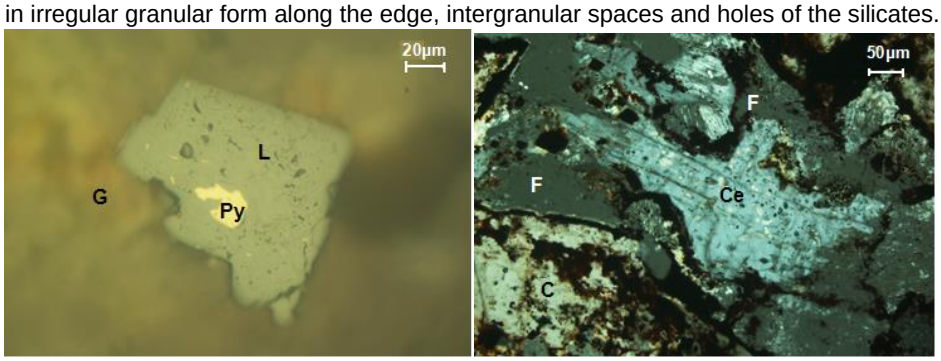

(a) (b)

Figure 5: (a) Limonite (L) included irregular fine pyrite (Py), G-gangue, reflect light; (b)Celesite (Ce) with orthogonal cleavage disseminated in fluorite (F), C-calcite, cross-polarized light

3.4 Disseminated grain size of the rare earth minerals

The grain size composition and distribution characteristics of the target mineral in the ores exerted great influences on the determination of the milling fineness and the establishment of a sound mineral processing flowsheet. MLA was used to count the disseminated grain sizes of the rare-earth minerals (including monazite, bastnaesite, parisite, ancylite, xenotime, calcium tornebohmite and loveringite) in the ores, the results were shown in Table 4.

Table 4: Disseminated grain sizes of the rare-earth minerals (%)

Grade (μm)	150-75	75-38	38-13	13-0
Distribution rate	26.72	32.81	30.64	9.83

As indicated in Table 4, the rare-earth minerals in the ores were in fine to micro granular grade, the fraction that had grain size < 0.038 mm took up a total of 40.47%. According to the analysis on disseminated grain size, the milling fineness should be <0.013 mm in order to confirm > 90% rare earth minerals occurred in single form.

4. Conclusion

The content of the rare-earth elements in the ores was 2.84%, the main rare earth minerals were bastnaesite (including parisite), and some minor monazite. The gangue minerals were commonly dolomite and apatite, and some minor celesite, calcite, quartz and fluorite. The occurrence states of the rare-earth minerals, such as bastnaesite and monazite, were similar, mainly disseminated along the edge, intergranular spaces, and cracks of dolomite, celesite, barite, apatite and quartz in sparse and scattered form, especially having close intergrowth relationship with dolomite. The rare-earth minerals had fine grain size, generally at 0.005-0.05 mm, <0.038 mm faction took up a total of around 40%. The rare-earth mineral may still have occurred in intergrowth form even if after fine milling process due to the fine grain size, high dispersion degree, and complicated embedded relationship with other minerals. The liberation degree of the rare-earth minerals was around 70% with the milling fineness of 95% passing 200 mesh (0.074 mm). The milling fineness should be <0.013 mm when processing the ores in order to confirm that the liberation degree was >90%, at which the rare-earth minerals were considered to reach sufficient liberation.

Acknowledgments

The author was funded by the National Natural Science Foundation of China (Project No. 51608192); the Natural Science Foundation of Hunan Province (Grant No. 2016JJ4031); the Open Research Fund Program of Key Laboratory of Metallogenic Prediction of Nonferrous Metals and Geological Environmental Monitoring (Central South University), Ministry of Education (Project No. 2016YSJS006); the Scientific Research Foundation for the Returned Overseas Chinese Scholars, State Education Ministry (Year 2015, No.1098).

Reference

Al-waisawy S., Jadwisienczak W.M., Wright J.T., Pendrill D., Rahman F., 2016, Laser excitation of red, green, blue and trichromatic white rare-earth phosphors for solid-state lighting applications, Journal of Luminescence, 169, Part A, 196-203, DOI: 10.1016/j.jlumin.2015.08.046

Che L.P., Yu Y.F, 2006., Mineral processing technology production status and development of rare earth ore in China, Chinese Rare Earths, 27(1), 95.

Frandrich R., Gu Y., Burrows D., 2007, Modern SEM- based mineral liberation analysis. International Journal of Mineral Processing, 84, 310- 320, DOI: 10.1016/j.minpro.2006.07.018

Gu Y., 2003, Automated scanning electron microscope based mineral liberation analysis. Journal of Minerals and Materials Characterization and Engineering, 2(1), 33- 41. DOI: 10.4236/jmmce.2003.21003

Hirajima T., Bissombolo A., Sasaki K., Nakayama K., Hirai H., Tsunekawa M., 2005, Floatability of rare earth phosphors from waste fluorescent lamps, International Journal of Mineral Processing, 77(4), 187-198, DOI: 10.1016/j.minpro.2005.05.002

Jaireth S., Hoatson D.M., Miezitis Y., 2014, Geological setting and resources of the major rare-earth-element deposits in Australia, Ore Geology Reviews, 62, 72-128, DOI: 10.1016/j.oregeorev.2014.02.008

Jordens A., Cheng Y.P., Waters K.E., 2013, A review of the beneficiation of rare earth element bearing minerals. Minerals Engineering, 41(1), 97-114, DOI: 10.1016/j.mineng.2012.10.017

Liu H.J., Feng Z.Y., Huang X.W., Long Z.Q., Wang M., Xiao Y.F., Hou Y.K., 2013, Study on purification and application of novel precipitant for ceria-based polishing powder. Journal of Rare Earths, 31(2), 174-179. DOI: 10.1016/S1002-0721(12)60254-3

Liu Q.H., Zhang S.H., Zheng H.Q, Wang J.F., Ren Q.Y., Zhao H., Yi Z., Huang J.G., 2015, Magnetic field simulation of helicon plasma thruster, Spacecr. Environmental Engineering, 32(3), 247-251.

Lucas J., Lucas P., Mercier T.L., Rollat A., Davenport W., 2015, Chapter 12-Polishing with rare earth oxides mainly cerium oxide CeO2, Rare Earths, 191-212, DOI: 10.1016/B978-0-444-62735-3.00012-7

Massari S., Ruberti M., 2013, Rare earth elements as critical raw materials: Focus on international markets and future strategies, Resources Policy, 38(1), 36-43, DOI: 10.1016/j.resourpol.2012.07.001

Sousa-Aguiar E.F., Trigueiro F.E., Zotin F.M.Z., 2013, The role of rare earth elements in zeolites and cracking catalysts, Catalysis Today, 218, 115-122, DOI: 10.1016/j.cattod.2013.06.021

Wallenstein D., Schäfer K., Harding R.H., 2015, Impact of rare earth concentration and matrix modification in FCC catalysts on their catalytic performance in a wide array of operational parameters, Applied Catalysis A General, 502, 27-41, DOI: 10.1016/j.apcata.2015.05.010

Xia G.Q., Wang D.X, Xue W.H., 2011, Progress on the research of helicon plasma thruster, Journal of Propulsion Technology, 32(6), 857-863.

Xu G.R., 1996. Conventional applications of the rare earth. Chinese Rare Earth, 20(3): 65-70.

Yu D.R., Wu Z.W., Peng E., 2005, Research status and development of the magnetic field design for stationary plasma thruster, Engineering Science, 7(4), 22-29.

Yu Q. M., Liu Y.F., Wu S., Lü X.D., Huang X.Y., Li X.X., 2008, Luminescent properties of Ca2SiO4: Eu3+ red phosphor for trichromatic white light emitting diodes, Journal of Rare Earths, 26(6), 783-786, DOI: 10.1016/S1002-0721(09)60005-3

Zhang P.S, 1989. A study on the genetic classification of rare earth mineral deposits of china, Chinese Journal of Geology, 1, 26-32.

Zhang Y.B., Gong M. L., Li H., 2007, Occurrence of REE in rare earthphosphorite in Zhijin area, Guizhou, Journal of Earth Sciences and Environment, 29(4), 362.

Zirner A.L.K., Marks M.A.W., Wenzel T., Jacob D.E., Markl G., 2015, Rare earth elements in apatite as a monitor of magmatic and metasomatic processes: The Ilímaussaq complex, South Greenland, Lithos, 228-229, 12-22, DOI: 10.1016/j.lithos.2015.04.013

Zouaoui A., Zili-Ghedira L., Nasrallah S., 2016, Experimental investigation of air dehumidification and regeneration operations using packed bed of silica gel particles, International Journal of Heat and Technology, 34(1), 103-109. DOI: 10.18280/ijht.340115